Antonie van Leeuwenhoek (2014) 106:431–438
DOI 10.1007/s10482-014-0211-7

ORIGINAL PAPER

Fumarate metabolism and ATP production in *Pseudomonas fluorescens* exposed to nitrosative stress

Varun P. Appanna · Christopher Auger · Sean C. Thomas · Abdelwahab Omri

Received: 30 April 2014 / Accepted: 3 June 2014 / Published online: 13 June 2014

Abstract Although nitrosative stress is known to severely impede the ability of living systems to generate adenosine triphosphate (ATP) via oxidative phosphorylation, there is limited information on how microorganisms fulfill their energy needs in order to survive reactive nitrogen species (RNS). In this study we demonstrate an elaborate strategy involving substrate-level phosphorylation that enables the soil microbe *Pseudomonas fluorescens* to synthesize ATP in a defined medium with fumarate as the sole carbon source. The enhanced activities of such enzymes as phosphoenolpyruvate carboxylase and pyruvate phosphate dikinase coupled with the increased activities of phospho-transfer enzymes like adenylate kinase and nucleoside diphophate kinase provide an effective strategy to produce high energy nucleosides in an O_2-independent manner. The alternate ATP producing machinery is fuelled by the precursors derived from fumarate with the aid of fumarase C and fumarate reductase. This metabolic reconfiguration is key to the survival of *P. fluorescens* and reveals potential targets against RNS-resistant organisms.

Keywords Energy production · Fumarate · Reactive nitrogen species (RNS) · *Pseudomonas fluorescens*

V. P. Appanna · C. Auger · S. C. Thomas · A. Omri (✉)
Department of Biology, Laurentian University, Sudbury, ON P3E2C6, Canada
e-mail: aomri@laurentian.ca

Introduction

Nitrosative stress occurs due to the uncontrolled formation of such reactive nitrogen species (RNS) as nitric oxide (NO), dinitrogen trioxide (N_2O_3), and peroxynitrite ($ONOO^-$). These RNS are generated intracellularly when NO reacts with hydrogen peroxide and superoxide. They are known to be toxic as these moieties react with sulphydryl groups, redox metals, heme residues and tyrosine-containing macromolecules (Quijano et al. 1997; Zielonka et al. 2012). Hence, nitrosative stress is known to severely impair oxidative phosphorylation (OP), a process that produces ATP in an O_2-dependent manner. This ATP-generating system relies on the tricarboxylic acid (TCA) cycle and the electron transport chain (ETC). While the former provides the reducing factors NADH and $FADH_2$, the latter aids in the shuttling of electrons to O_2, the terminal electron acceptor (Lemire et al. 2012). Numerous enzymes that participate in these metabolic networks require heme and Fe–S clusters for proper functioning and are rendered ineffective by RNS (Auger et al. 2011; Poole 2005). Hence it is not surprising that numerous microbes have developed mechanisms to deal with these toxic RNS. Their conversion into innocuous nitrate, and the upregulation of enzymes dedicated to the removal of nitrosylated moieties, a common occurrence during nitrosative stress, are two strategies invoked by some bacteria (Auger et al. 2011). Although the detoxification mechanisms aimed at RNS have been studied,

there is a dearth of information on how RNS-tolerant microbes satisfy their ATP requirements.

Substrate level phosphorylation (SLP) is the other ATP-producing machine that is commonly utilized by biological systems. High energy compounds that are obtained following various biochemical transformations help phosphorylate adenosine monophosphate (AMP) and/or adenosine triphosphate (ADP) into ATP (Kim et al. 2013). These compounds include phosphoenolpyruvate (PEP) and 1,3,biphosphoglycerate, that are products of glycolysis, as well as succinyl CoA which is produced during the TCA cycle (Han et al. 2013; Singh et al. 2009). Pyruvate kinase is a key enzyme that converts PEP into ATP in the presence of ADP (Auger et al. 2012, 2013). Some bacteria are also known to possess the acetate kinase-phophotransacetylase system that is involved in the processing of acetyl CoA into ATP (Hunt et al. 2010; Ingram-Smith et al. 2006).Although ATP formation mediated by SLP is widespread in nature, the metabolic networks that are utilized to fulfill the need for this universal energy currency under environmental stress along with its regulation have yet to be fully elucidated.

As part of our efforts to decipher the metabolic adaptations that allow the soil microbe *Pseudomonas fluorescens* to survive in extreme environments (Auger et al. 2011), we have evaluated how this nutritionally-versatile microbe fulfills its requirements for ATP, under a nitrosative challenge. This condition is known to render OP ineffective. In this study fumarate a TCA cycle intermediary and a dicarboxylic acid that is usually metabolized by RNS-sensitive Fe–S cluster rich enzymes was utilized as the sole source of carbon. The ability of *P. fluorescens* to elaborate an alternate-ATP generating network and the metabolism of fumarate are described. The significance of these findings in combatting RNS-resistant microbes is also discussed.

Materials and methods

Bacterial growth conditions

Pseudomonas fluorescens, strain ATCC 13525, was grown in a phosphate growth medium containing Na_2HPO_4 (6 g), KH_2PO_4 (3 g), NH_4Cl (0.8 g), $MgSO_47H_2O$ (0.2 g), and fumarate (2.25 g) per 1 liter of distilled and deionized water. One mL of trace elements was added per liter of medium as described in Bignucolo et al. (2013). Nitrosative stress was achieved with the addition of sodium nitroprusside (SNP) at a concentration of 10 mM (Auger et al. 2011). Cultures pH was adjusted to 6.8 using dilute NaOH. Previous studies have shown that *P. fluorescens* has the ability to reach its optimal growth at this pH (Auger et al. 2011). The mixtures were then transferred to 500 mL Erlenmeyer flasks. Each flask was filled with 200 mL of medium. Cultures were inoculated by adding 1 mL of stationary phase bacteria to the growth media. These cultures were aerated on a gyrator water bath shaker (Model 76, New Brunswick Scientific). Once the stationary phase was reached, portions of samples were centrifuged at 10,000×*g* for 10 min at 4 °C. Aliquots (10 mL) of spent fluid were stored for further experiments. Washing of the bacterial pellet was then completed using 0.85 % NaCl, and the pellet was re-suspended using a cell storage buffer (50 mM Tris–HCl, 5 mM $MgCl_2$, and 1 mM phenylmethylsulphonyl fluoride, pH 7.3). Membranous and soluble cellular fractions were obtained by sonication and centrifugation of the disrupted cells (al-Aoukaty et al. 1992). Bradford assays were performed on both fractions in triplicate to determine protein concentration. These fractions were kept at 4 °C for 5 days or at −20 °C for 4 weeks for further study.

RNS-detoxifying enzymes and functional metabolomic studies

To evaluate the impact of the nitrosative stress on the bacterium, cultures were grown in control and nitrosative stressed-conditions at various time intervals and cellular yield was assessed by Bradford assay (Bradford 1976). Fumarate consumption was monitored by high performance liquid chromatography (HPLC) at a wavelength of 236 nm (Charoo et al. 2014). The presence of nitrate reductase and nitrite reductase were also probed to determine the relative activity of these detoxifying enzymes in each system. In gel activity of the enzymes was monitored and densitometric readings were recorded to obtain relative activities (Auger et al. 2011). The Griess assay was performed on the spent fluids from both control and RNS-stressed cultures in order to determine relative content of nitrate and nitrite respectively (Miranda et al. 2001).

To assess significant metabolite level differences in control and RNS-exposed cultures, HPLC was

performed on the spent fluids and soluble fractions of. Two mg/mL of protein equivalent of the cell cell-free extract (CFE) were taken and heated gently to ensure precipitation of proteins and lipids (Mailloux et al. 2011). The supernatants were subsequently monitored at 210 and 254 nm respectively. All metabolite levels were compared to known compounds, and by spiking with the appropriate standards (Auger et al. 2011).

Analyses of TCA cycle and ETC enzymes

Blue native polyacrylamide gel electrophoresis (BN-PAGE) was performed to detect relative activity of enzymes in control and stressed cultures involved in the TCA cycle and in the ETC. Proteins were prepared for BN-PAGE by dilution with native buffer (50 mM Bis–Tris, 500 mM ε-aminocaproic acid, pH 7.0, 4 °C) until proteins were at a concentration of 4 mg/mL. One % (v/v) β-dodecyl-D-maltoside was added to the membranous fractions to help in the solubilization of the proteins. Once the gel had finished separation, it was placed in a reaction buffer (25 mM Tris–HCl, 5 mM MgCl2, at pH 7.4) for 15 min to rinse off buffers. Once completed, specific protein fractions were separated and placed in their appropriate reaction mixtures where enzyme reactions were performed. All reactions were based on the presence of a pink formazan precipitate, formed during reduction reactions (Schagger and von Jagow 1991; Han et al. 2012).

NAD^+-dependent isocitrate dehydrogenase (ICDH-NAD^+) activity was visualized using a reaction mixture containing 5 mM isocitrate, 0.5 mM NAD^+, 0.2 mg/mL PMS and 0.4 mg/mL INT. For malate dehydrogenase (MDH) malate was used as the substrate for the reaction. Complex II was detected by the addition of 0.5 mM FAD^+, and 0.4 mg/mL INT with 5 mM succinate. Complex IV was probed using diaminobenzidine (10 mg/mL), cytochrome C (10 mg/mL), sucrose (562.5 mg/mL). In the case of both ETC complexes probed, the reaction were made in reaction buffer with the addition of 5 mM of KCN. Appropriate negative controls consisted of reaction mixtures that did not contain the substrate or cofactors for the reaction. For example, reaction mixtures devoid of isocitrate and/or NAD^+ were utilized as negative controls for ICDH-NAD^+ while the commercial enzyme was tested as a positive control. Once completed all of the above reactions were destained using 40 % methanol, 10 % glacial acetic acid. Activity bands were quantified using ImageJ for Windows. Proper protein loading was determined by Coomassie staining for total proteins. Equal amounts of proteins (60 μg) were loaded in the respective lanes. Following the appearance of the activity bands (at the same time), the bands were excised and incubated in the reaction mixture to monitor the products formed. Enzymes such as malate dehydrogenase (MDH) and pyruvate carboxylase (PC) that had similar activity in the control and stressed cultures were utilized as internal controls. Unless otherwise mentioned, all comparative experiments were performed at the late logarithmic phase of growth. Select activity bands were excised and incubated in the appropriate reaction mixtures. The substrates and products of these mixtures were detected by HPLC.

Fumarate metabolism and ATP synthesizing enzymes

In an effort to evaluate how fumarate was metabolized the cell-free extract (2 mg/mL protein equivalent) was incubated with 2 mM of fumarate in the presence or absence of KCN (5 mM). The soluble cell free extract (2 mg/mL) was also incubated with 2 mM oxaloacetate, 1 mM PP_i, and 0.5 mM AMP in order to determine how ATP was being generated. These reactions were performed with and without KCN. The production of ATP and other metabolites was monitored by HPLC. Fumarase was identified by in-gel activity assay using a reaction mixture containing 5 mM fumarate, 5 units/mL of malate dehydrogenase, 0.5 mM NAD^+, 0.2 mg/mL PMS and 0.4 mg/mL INT. The two isoforms of fumarase A and C were detected with the aid of inhibitors as described in Chénier et al. (2008). Fumarate reductase (FRD) was also probed using succinate and NAD^+ (Watanabe et al. 2011). The activity of, pyruvate carboxylase (PC), was ascertained by utilizing enzyme-coupled assays as described (Singh et al. 2005). Pyruvate phosphate dikinase (PPDK) was monitored using a reaction mixture consisting of 5 mM PEP, 0.5 mM AMP, 0.5 mM sodium pyrophosphate (PP_i), 0.5 mM NADH, 10 units of LDH, 0.0167 mg/mL of DCIP and 0.4 mg/mL of INT. Adenylate kinase (AK) was detected by an enzyme-coupled assay involving hexokinase and glucose-6-phosphate dehydrogenase (G6PDH). The ability of the enzyme to convert ADP to ATP enabled the conversion of glucose into glucose-6-phosphate that was then detected by the precipitation of formazan in the gel. Nucleoside diphosphate kinase

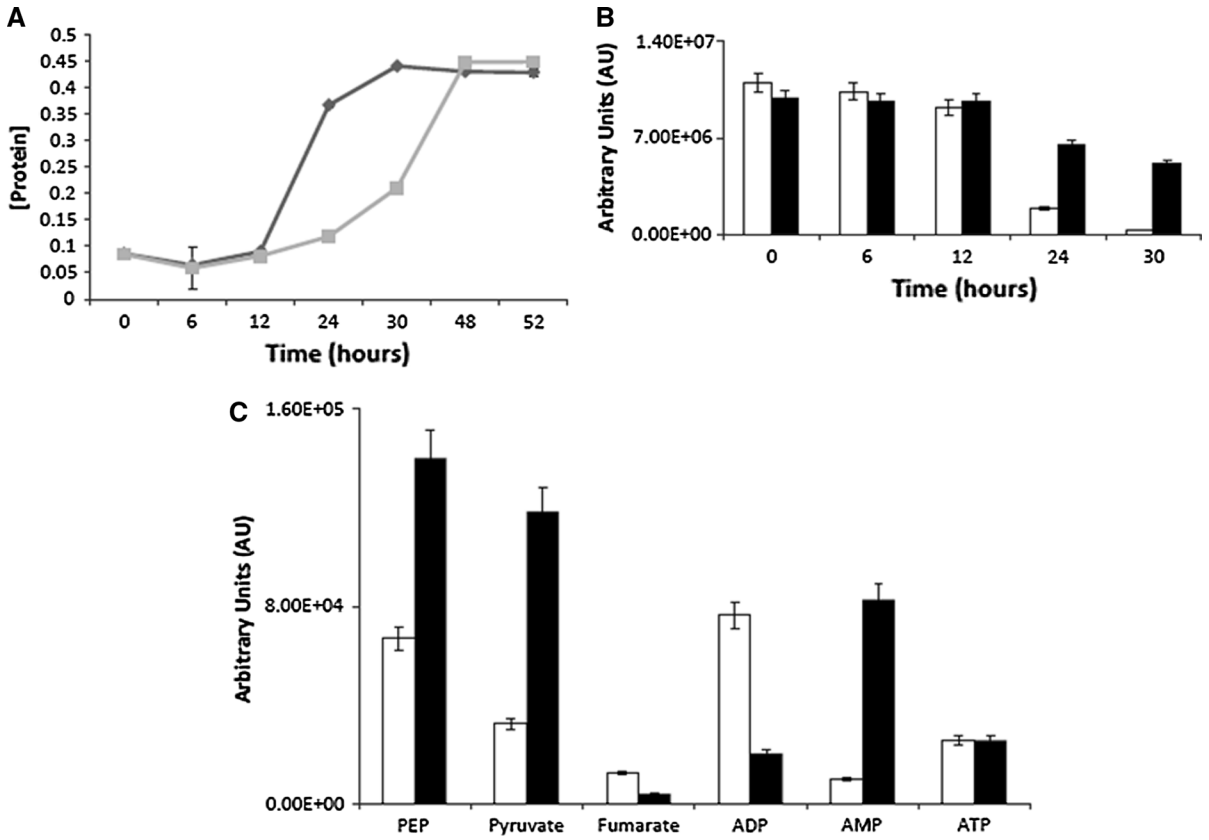

Fig. 1 Effects of nitrosative stress on *P. fluorescens*, **a** growth profiles of control and RNS-stressed cultures, **b** fumarate consumption in control and stressed cultures as measured with HPLC at 236 nm. n = 3. (SD AU ±), **c** select metabolites and nucleotides in the soluble cell free extract (sCFE). *White bar* control, *black bar* stressed cultures (n = 3; SD ±)

(NDPK) in gel assay, was performed as described in Mailloux et al. (2008). These bands were excised and their activities were followed by HPLC. Spectrophotometric analyses were also performed to confirm the activities of some select enzymes. MDH and ICDH-NAD^+ dependent were monitored by following the formation of NADH at 340 nm in the CFE in the presence of their respective substrates (Auger et al. 2011).

Data were expressed as a ± standard deviation. Statistical correlations and significance of data were all confirmed using the Student T test ($p \leq 0.05$). All experiments were performed at least twice snd in triplicate.

Results and discussion

When *P. fluorescens* was exposed to nitrosative stress in a defined phosphate medium with fumarate as the sole source of carbon, the biomass at the stationary phase of growth was similar to that of the control culture. Although growth rate was slower in the stressed cultures, fumarate was utilized at a faster rate (Fig. 1). The impact of nitrosative stress was evident in the stressed bacteria, as there was an increase of 18 and 13 fold in activity of nitrite and nitrate reductase respectively. The presence of elevated levels of nitrate and nitrite in the spent fluid indicated that RNS was also being detoxified (Table 1). The disparate metabolic profiles observed in the soluble CFE between control and stressed cultures at the same phase of growth indicated a shift in metabolic pathways. Peaks attributed to pyruvate, PEP and AMP were also more intense in the bacteria obtained from the RNS-exposed cultures. The control cultures had higher levels of ADP (Fig. 1).

As there was a stark difference in these nucleoside phosphate levels, it became apparent that the ATP-

Table 1 Activities of some enzymes, and nitrate and nitrite levels in control and stressed cultures

Experiment	Control	stress
Nitrate reductase activity (AU)[a]	3,597 ± 58	46,501 ± 49
Nitrite reductase activity (AU)[a]	2,113 ± 62	37,632 ± 197
Griess assay (NO_2^-)	2.10 ± 0.63 μM	102 ± 15 μM
Griess assay (NO_3^-)	2.78 ± 0.71 μM	113 ± 22 μM
ICDH-NAD[4] activity (nmol NADH formed/min/mg protein)[b]	106.67 ± 10.4	33.55 ± 2.1
MDH activity (nmol NADH formed/min/mg protein)[b]	60.43 ± 5.5	56.13 ± 3.2

[a] In gel activity was monitored using densitometric reading (n = 3)

[b] NADH levels monitored at 340 nm. Produced using processed protein mixed with appropriate substrates

producing machinery had been affected. Analysis of select TCA cycle enzymes and the ETC revealed that ICDH-NAD^+ dependent, Complex II and Complex IV decreased in RNS-exposed bacteria. MDH did not appear to change in the control and stressed cultures (Fig. 2). Indeed the activity of ICDH-NAD^+ was about 3 fold higher in the control compared to the stressed cultures as measured spectrophotometrically. MDH activity was found to be similar in these two conditions (Table 1). Hence, it was important to discern how ATP was generated since the TCA cycle and ETC enzymes were ineffective in the stressed cultures. When the CFE of the control and stressed *P. fluorescens* were incubated with fumarate in the presence of KCN, a potent inhibitor of OP, ATP production was severely decreased in the control. However, ATP levels in the CFE obtained from the RNS-challenged cells remained relatively similar with and without the presence of KCN. This indicated that *P. fluorescens* was utilizing an alternate metabolic network, independent of OP, to generate ATP in an effort to combat the toxic influence of the nitrosative stress (Fig. 2).

Fumarate is usually metabolized by fumarase, an enzyme known to be sensitive to oxidative and nitrosative stress (Lushchak et al. 2014,). In this instance, *P. fluorescens* upregulated the activity of fumarase C, an isoenzyme known to be less prone to nitrosative stress. Two bands were evident in the electrophoregram obtained from BN-PAGE analysis (Fig. 3). FRD, another enzyme involved in fumarate metabolism was prominent in the stressed cells while the activity band attributable to this enzyme was barely discernable in the control cells (Fig. 3). Hence, Fum C and FRD were utilized to degrade fumarate in the stressed bacteria. The presence of elevated amounts of phosphoenol pyruvate (PEP) in the CFE of the stressed cultures, led us to analyze enzymes responsible for the production of this metabolite. PEPC, an enzyme known to mediate the

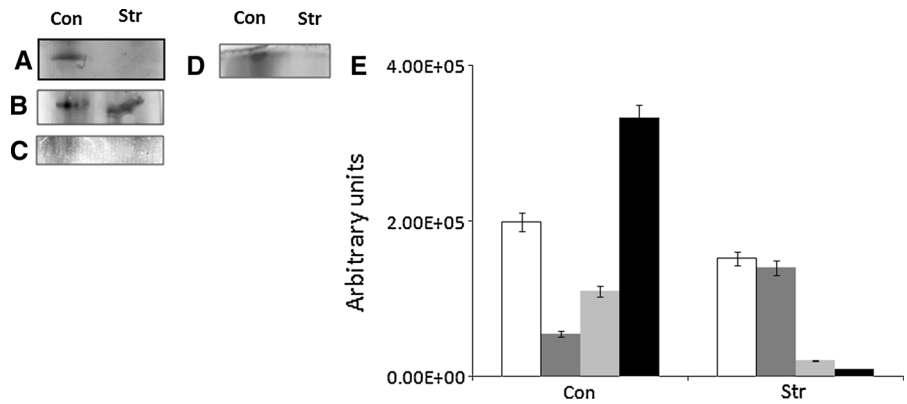

Fig. 2 Enzymatic activity of select TCA cycle and ETC enzymes: **a** ICDH-NAD^+, **b** MDH, **c** Complex II, **d** Complex IV (*Con* control, *Str* stress): **e** fumarate metabolism in *P. fluorescens* (n = 3). *white bar* ATP without KCN, *dark gray bar*: ATP with KCN, *light gray bar* fumarate consumption without KCN, *black bar* fumarate consumption with KCN. *Con* control, Str stress

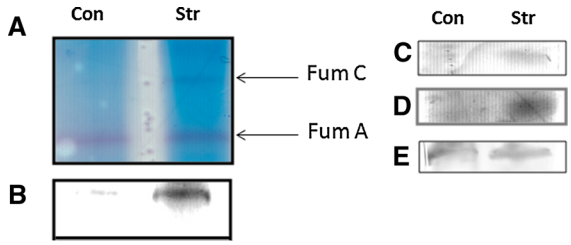

Fig. 3 Enzymes involved in fumarate metabolism; **a** fumarase isoforms *Fum A* and *Fum C*, **b** fumarate reductase (FRD), **c** phosphoenolpyruvate carboxylase (PEPC), **d** pyruvate phosphate dikinase (PPDK), **e** pyruvate carboxylase (PC)

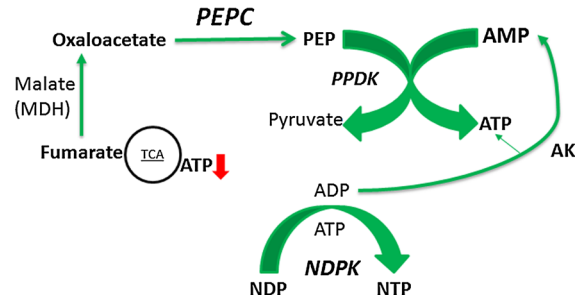

Fig. 5 An alternate ATP-producing machinery in *P. fluorescens* exposed to nitrosative stress. Fumarate and AMP are key ingredients in this process

transformation of oxaloacetate into PEP, was increased as was PPDK (Fig. 3). The former utilizes inorganic phosphate (P_i) while the latter invokes the participation of PEP, AMP and PP_i to form pyruvate and ATP. This metabolic arrangement would provide an effective means of producing ATP in an O_2-independent manner. Indeed similar ATP-generating networks have been uncovered in infectious organisms (Adam 2001; Couston et al. 2003; Hall and Ji 2013: Ma et al. 2013). However, it was important to evaluate the biochemical processes involved in the fixation of ATP and the formation of AMP, a feature critical for this energy-generating machinery to work efficiently via substrate-level phosphorylation.

Adenylate kinase (AK), an enzyme that orchestrates the synthesis of ATP from ADP produces AMP, while NDPK is able to transfer the high energy phosphate from ATP to NDP or dNDP. Indeed both of these enzymes were found to have enhanced activities in the culture obtained from the stressed media compared to the control (Fig. 4). When the activity band was excised and incubated with the respective substrate, the formation of ATP and AMP from ADP in the case of AK was evident. The excised activity band of NDPK readily gave peaks indicative of ATP and GDP when incubated with ADP and GTP (Fig. 4). To confirm the workings of this metabolic network oxaloacetate, a product of fumarate, AMP, and PP_i were incubated with the soluble CFE from stressed and control bacteria obtained at the same phase of growth. Peaks attributed to PEP, GTP, and ATP, in the

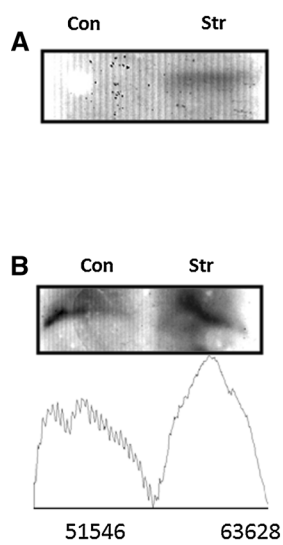

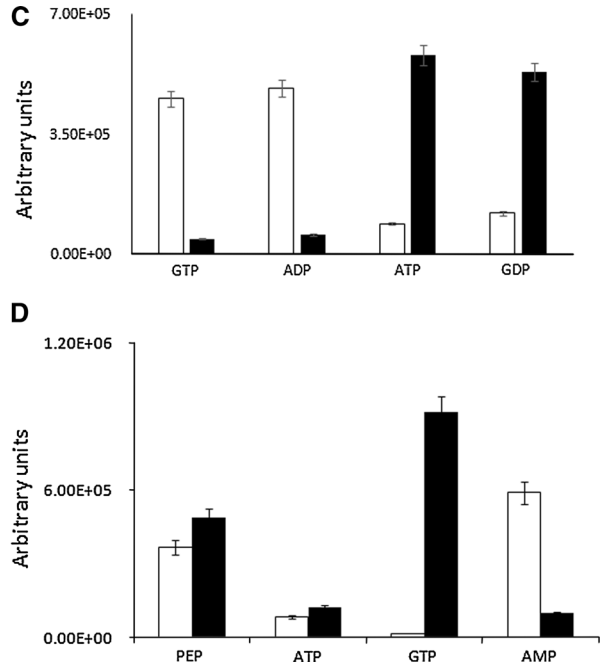

Fig. 4 **a** Adenylate Kinase activity, **b** NDPK activity, activity band and densitometric readings for in gel activity (n = 3) (*Con* control, *Str* stress) bands were incubated with ADP and GTP. C Production of significant nucleotides with reaction mixture containing GTP and ADP after 30 min of incubation (*white bar* control, *black bar* stress) n = 3. **d** Nucleoside triphosphate production by CFE in the presence of oxaloacetate, AMP, PP_i. (*Con* control, *Str* stress) n = 3 (SD AU ±) (*white bar* control, *black bar* Stress)

CFE isolated from the stressed *P. fluorescens* provided elegant evidence for the energy generating machine that was responsible for fuelling the survival of the stressed bacteria challenged by nitrosative stress (Fig. 5).

Although the detoxification mechanisms involved in nitrosative stress have been subject to numerous investigations, the molecular pathways involved in the maintenance of ATP homeostasis under these conditions have yet to be fully unravelled. This study shows that *P. fluorescens* elaborates an intricate network to fulfill its energy needs. The pivotal role of the TCA cycle in generating ATP by substrate-level phosphorylation in *P. fluorescens* exposed to aluminum toxicity was recently demonstrated (Singh et al. 2009). In this instance the upregulation of ICDH-NADP dependent and isocitrate lyase allows to combat the ineffectiveness of the Al-sensitive aconitase in order to generate glyoxylate and NADPH. The former then is transformed into oxalate and ATP, a process that is mediated by acylating glyoxylate dehydrogenase, oxalate CoA-transferase and succinyl-CoA synthetase. NADH and NADPH levels are also intricately modulated during stress (Mailloux et al. 2011; Li et al. 2014). In this study, PPDK in tandem with the phosphotransfer systems involving AK and NDPK, provides an efficient route to ATP with the concomitant formation of AMP and NTP. Indeed, infectious organisms that are subjected to the defense mechanisms of their host are known to invoke SLP, using PPDK to produce ATP. Strategies to inhibit these enzymes may provide therapeutic cues against these microbes. In conclusion, findings in this report further reveal the nutritional versatility and adaptability of *P. fluorescens* and demonstrate the intricate metabolic network it utilizes to fulfill its requirements for ATP when subjected to nitrosative stress. The metabolic module may be a practical target to arrest infectious organisms known to invoke this pathway to thwart host defenses.

References

Adam RD (2001) Biology of *Giardia lamblia*. Clin Microbiol Rev 14:447–475

al-Aoukaty A, Appanna VD, Falter H (1992) Gallium toxicity and adaptation in *Pseudomonas fluorescnes*. FEMS Microbiol Lett 71:265–272

Auger C, Lemire J, Cecchini D, Bignucolo A, Appanna VD (2011) The metabolic reprogramming evoked by nitrosative stress triggers the anaerobic utilization of citrate in *Pseudomonas fluorescens*. PLoS ONE 6:e28469

Auger C, Appanna V, Castonguay Z, Han S, Appanna VD (2012) A facile electrophoretic technique to monitor phosphoenolpyruvate-dependent kinases. Electrophoresis 33:1095–1101

Auger C, Han S, Appanna VP, Thomas SC, Ulibarri G, Appanna VD (2013) Metabolic reengineering invoked by microbial systems to decontaminate aluminum: implications in bioremediation technologies. Biotechnol Adv 31:266–273

Bignucolo A, Appanna VP, Thomas SC, Auger C, Han S, Omri A, Appanna VD (2013) Hydrogen peroxide stress a metabolic reprogramming in *Pseudomonas fluorescens*: enhanced production of puyruvate. J Biotechnol 167:309–315

Bradford MB (1976) A rapid and sensitive method for the quantitation of microgram quantities of protein utilizing the principle of protein-dye binding. Anal Biochem 72:248–254

Charoo NA, Shamsher AAA, Lian LY, Abrahamsson B, Cristofoletti R, Groot DW, Kopp S, Langguth P, Polli J, Shah VP, Dressman J (2014) Biowaiver monograph for immediate-release solid oral dosage forms: bisoprolol fumarate. J Pharma Sci 103:378–391

Chénier D, Bériault R, Mailloux R, Baquie M, Abramia G, Lemire J, Appanna VD (2008) Metabolic adaptation in *Pseudomonas fluorescens* evoked by aluminum and gallium toxicity: involvement of fumarase C and NADH oxidase. Appl Environ Microbiol 74:3977–3984

Couston V, Besterio S, Biran M, Diolez P, Bouchaud V, Voisin P, Michels PAM, Canioni P, Baltz T, Bringaud F (2003) ATP generation in the *Trypanosoma brucei* procyclic form cytosolic substrate level phosphorylation is essential, but not oxidative phosphorylation. J Biol Chem 278:49625–49635

Hall JW, Ji Y (2013) Sensing and adapting to anaerobic conditions by *Staphylococcus aureus*. Adv Appl Microbiol 84:1–25

Han S, Auger C, Castonguay Z, Appanna VP, Thomas SC, Appanna VD (2012) The unravelling of metabolic dysfunctions linked to metal-associated diseases by blue native polyacrylamide gel electrophoresis. Anal Bioanal Chem 405(6):1821-1831

Han S, Auger C, Thomas SC, Beites CL, Appanna VD (2013) Mitochondrial biogenesis and energy production in differentiating stem cells: a functional metabolic study. Cell Reprogram 16:84–90

Hunt KA, Flynn JM, Naranjo B, Shikhare ID, Gralnick JA (2010) Substrate-level phosphorylation is the primary source of energy conservation during anaerobic respiration of *Shewanella oneidensis* strain MR-1. J Bacteriol 192:3345–3351

Ingram-Smith C, Martin SR, Smith KS (2006) Acetate kinase: not just a bacterial enzyme. Trends Microbiol 14:249–253

Kim D, Yu BJ, Kim JA, Lee Y, Choi S, Kang S (2013) The acetylproteome of Gram-positive model bacterium *Bacillus subtilis*. Proteomics 13:1726–1736

Lemire J, Auger C, Bignucolo A, Appanna VP, Appanna VD (2012) Metabolic strategies deployed by *Pseudomonas*

fluorescens to combat metal pollutants: biotechnological prospects in current research, technology and education topics in applied microbiology and microbial biotechnology. In: Mendez-vilas A (ed). Formalex Publisher, pp 177–187

Li K, Pidatala RV, Shaik R, Datta R, Ramakrishna W (2014) Integrated metabolomic and proteomic approaches dissect the effect of metal-resistant bacteria on maize biomass and copper uptake. Environ Sci Technol 48:1184–1193

Lushchak OV, Piroddi M, Galli F, Lushchak VI (2014) Aconitase post-translational modification as a key in linkage between Krebs cycle, iron homeostasis, redox signaling, and metabolism of reactive oxygen species. Redox Rep 19:8–15

Ma Y, Guo C, Li H, Peng X (2013) Low abundance of respiratory nitrate reductase is essential for *Escherichia coli* in resistance to aminoglycoside and cephalosporin. J Proteom 87:78–88

Mailloux RJ, Darwich R, Lemire J, Appanna V (2008) The monitoring of nucleotide diphosphate kinase activity by blue native polyacrylamide gel electrophoresis. Electrophor 29:1484–1489

Mailloux RJ, Lemire J, Appanna VD (2011) Metabolic networks to combat oxidative stress in *Pseuodomonas fluorescens*. Antonie Van Leeuwenhoek 99:433–442

Miranda KM, Espey MG, Wink DA (2001) A rapid, simple spectrophotometric method for simultaneous detection of nitrate and nitrite. Nitric Oxide 5:62–71

Poole RK (2005) Nitric oxide and nitrosative stress tolerance in bacteria. Biochem Soc Trans 33:176–180

Quijano C, Alvarez B, Gatti RM, Augusto O, Radi R (1997) Pathways of peroxynitrite oxidation of thiol groups. Biochem J 322:167–173

Schagger H, von Jagow G (1991) Blue native electrophoresis for isolation of membrane protein complexes in enzymatically active form. Anal Biochem 199:223–231

Singh R, Chenier D, Beriault R, Mailloux R, Hamel RD, Appanna VD (2005) Blue native polyacrylamide gel electrophoresis and the monitoring of malate- and oxaloacetate-producing enzymes. J Biochem Biophys Methods 64:189–199

Singh R, Lemire J, Mailloux RJ, Chénier D, Hamel R, Appanna VD (2009) An ATP and oxalate generating variant tricarboxylic acid cycle counters aluminum toxicity in Pseudomonas fluorescens. PloS One 4:e7344

Watanabe S, Zimmerman M, Goodwin MB, Sauer U, Barry CE, Boshoff HI (2011) Fumarate reductase activity maintains an energized membrane in anerobic *Mycobacterium tuberculosis*. PLoS ONE 7:1–15

Zielonka J, Zielonka M, Sikora A, Adamus J, Joseph J, Hardy M, Ouari O, Dranka BP, Kalyanarama B (2012) Global profiling of reactive oxygen and nitrogen species in biological systems: high-throughput real-time analyses. J Biol Chem 287:2984–2995